Synthesis and Characterization of the Mixed-Valence Diamagnetic Two-Electron-Reduced Isopolytungstate $[W_{10}O_{32}]^{6-}$. Evidence for an Asymmetric d-Electron Distribution over the Tungsten Sites

Dean C. Duncan[†] and Craig L. Hill*

Department of Chemistry, Emory University, Atlanta, Georgia 30322

Received February 29, 1996[⊗]

The synthesis of the *unprotonated* two-electron-reduced isopolytungstate $[W_{10}O_{32}]^{6-}$ (**2**) is reported here. Additionally, full experimental details are given for the acquisition of both high signal-to-noise and integrable natural-abundance ^{17}O NMR spectra of polyoxometalates. Titration of an acetonitrile solution containing **2** with 0.13 M triflic acid is followed by UV−visible/near-IR spectroscopy. The spectra reveal isosbestic points which are consistent with five distinct protonation states, H_x**2**, where $x = 0-4$. Similar to a reported mixture of H_x**2** species ($x = 1-2$), **2** is EPR silent over the temperature range 4−300 K and is effectively diamagnetic. The ^{17}O and ^{183}W NMR spectra of **2** both indicate retention of the overall structure and symmetry (D_{4h}) of the oxidized d^0 precursor complex $[W_{10}O_{32}]^{4-}$ (**1**), and both spectra are consistent with delocalization of the two d electrons on the NMR time scale. The relative ^{17}O electric field gradients (efg) between **1** and **2** for the same oxygen site (*e.g.* O_a(**2**)/O_a(**1**) for site a) were deduced from ^{17}O line width measurements. These data are consistent with an increase in covalency for all three types of W−O−W bonds in **2** relative to **1**. ^{183}W NMR chemical shift and T_1 measurements indicate that the d electron density in **2** is located primarily on the equatorial tungsten sites. Similarly, the location of the two d electrons in the reduced Wells−Dawson heteropolytungstate α-$[P_2W_{18}O_{62}]^{8-}$ also is reported to be on the equatorial sites. Both **2** and α-$[P_2W_{18}O_{62}]^{8-}$ are the only known diamagnetic W^V-site "pure-addenda" (isometal) polyoxometalates which exhibit an asymmetric d-electron distribution over the metal sites.

Introduction

Polyoxometalates comprise a class of d^0 metal complexes of the group VB and VIB elements (excluding Cr) and exhibit both diverse and tunable domains of sizes, shapes, charge densities, acidities, and reversible redox potentials.[1−7] Polyoxometalates in their reduced states form a potentially important class of mixed-valence compounds commonly referred to as "blues" or "heteropoly blues" owing to their intense blue color. These complexes generally are paramagnetic when reduced by an odd number of electrons and are diamagnetic when reduced by an even number of electrons. Numerous papers have been published addressing the properties of these mixed-valence species.[8−45]

The structure of the d^0 decatungstate isopolyanion $[W_{10}O_{32}]^{4-}$ (**1**) is illustrated in Figure 1. It consists of two defect Lindquist ($[W_5O_{14}]^{2-}$) fragments linked by four corner-sharing oxygens with an unusually wide W−O−W angle of 178°.[46] Each

[†] Present address: Department of Chemistry, University of Texas, Austin, TX 78712

[⊗] Abstract published in *Advance ACS Abstracts,* September 15, 1996.

(1) References 2−7 are reviews on polyoxometalates.
(2) Pope, M. T. *Heteropoly and Isopoly Oxometalates*; Springer-Verlag: Berlin, 1983.
(3) Day, V. W.; Klemperer, W. G. *Science* **1985**, *228*, 533−541.
(4) Pope, M. T.; Müller, A. *Angew. Chem., Int. Ed. Engl.* **1991**, *30*, 34−48.
(5) Pope, M. T.; Müller, A. *Mol. Eng.* **1993**, *3*, 1−8.
(6) *Polyoxometalates: From Platonic Solids to Anti-retroviral Activity*; Pope, M. T., Müller, A., Eds.; Kluwer Academic Publishers: Dordrecht, Netherlands, 1993.
(7) Müller, A. *J. Mol. Struct.* **1994**, *325*, 13−35.
(8) Launay, J. P. *J. Inorg. Nucl. Chem.* **1976**, *38*, 807−816.
(9) Sanchez, C.; Livage, J.; Launay, J. P.; Fournier, M.; Jeannin, Y. *J. Am. Chem. Soc.* **1982**, *104*, 3194−3202.
(10) Sanchez, C.; Livage, J.; Launay, J. P.; Fournier, M. *J. Am. Chem. Soc.* **1983**, *105*, 6817−6823.
(11) Chemseddine, A.; Sanchez, C.; Livage, J.; Launay, J. P.; Fournier, M. *Inorg. Chem.* **1984**, *23*, 2609−2613.
(12) Chemseddine, A. *J. Non-Cryst. Solids* **1992**, *147*, 313−319.
(13) Kozik, M.; Hammer, C. F.; Baker, L. C. W. *J. Am. Chem. Soc.* **1986**, *108*, 2748−2749.
(14) Kozik, M.; Hammer, C. F.; Baker, L. C. W. *J. Am. Chem. Soc.* **1986**, *108*, 7627−7630.
(15) Kozik, M.; Baker, L. C. W. *J. Am. Chem. Soc.* **1987**, *109*, 3159−3160.
(16) Kozik, M.; Casañ-Pastor, N.; Hammer, C. F.; Baker, L. C. W. *J. Am. Chem. Soc.* **1988**, *110*, 7697−7701.
(17) Kozik, M.; Baker, L. C. W. *J. Am. Chem. Soc.* **1990**, *112*, 7604−7611.
(18) Casañ-Pastor, N.; Gomez-Romero, P.; Jameson, G. B.; Baker, L. C. W. *J. Am. Chem. Soc.* **1991**, *113*, 5658−5663.
(19) Casañ-Pastor, N.; Baker, L. C. W. *J. Am. Chem. Soc.* **1992**, *114*, 10384−10394.
(20) Kozik, M.; Baker, L. C. W. In *Polyoxometalates: From Platonic Solids to Anti-retroviral Activity*; Pope, M. T., Müller, A. Eds.; Kluwer Academic Publishers: Dordrecht, The Netherlands, 1993; pp 191−202.
(21) Kirby, J. F.; Baker, L. C. W. *J. Am. Chem. Soc.* **1995**, *117*, 10010−10016.
(22) Harmalker, S. P.; Pope, M. T. *J. Am. Chem. Soc.* **1981**, *103*, 7381−7383.
(23) Harmalker, S. P.; Leparulo, M. A.; Pope, M. T. *J. Am. Chem. Soc.* **1983**, *105*, 4286−4292.
(24) Barrows, J. N.; Jameson, G. B.; Pope, M. T. *J. Am. Chem. Soc.* **1985**, *107*, 1771−1773.
(25) Piepgrass, K.; Pope, M. T. *J. Am. Chem. Soc.* **1987**, *109*, 1586.
(26) Piepgrass, K.; Barrows, J. N.; Pope, M. T. *J. Chem. Soc., Chem. Commun.* **1989**, 10−12.
(27) Barrows, J.; Pope, M. T. In *Electron Transfer in Biology and the Solid State*; King, R. B., Kurtz, D. M., Jr., Kutal, C., Norton, M. L., Scott, R. A., Eds.; Advance in Chemistry 226; American Chemical Society: Washington, DC, 1990; Chapter 21.
(28) Barrows, J. N.; Pope, M. T. *Inorg. Chim. Acta* **1993**, *213*, 91−98.
(29) Yamase, T. *Polyhedron* **1986**, *5*, 79.
(30) Yamase, T. *J. Chem. Soc., Dalton Trans.* **1987**, 1597.
(31) Yamase, T.; Usami, T. *J. Chem. Soc., Dalton Trans.* **1988**, 183.
(32) Yamase, T.; Suga, M. *J. Chem. Soc., Dalton Trans.* **1989**, 661.
(33) Yamase, T. *J. Chem. Soc., Dalton Trans.* **1991**, 3055.
(34) Fournier, M.; Rocchiccioli-Deltcheff, C.; Kazansky, L. P. *Chem. Phys. Lett.* **1994**, *223*, 297−300.
(35) Cooper, J. B.; Way, D. M.; Bond, A. M.; Wedd, A. G. *Inorg. Chem.* **1993**, *32*, 2416−2420.
(36) Borshch, S. A.; Bigot, B. *Chem. Phys. Lett.* **1993**, *212*, 398−402.
(37) Borshch, S. A. *THEOCHEM* **1995**, *330*, 139−143.
(38) Barra, A. L.; Gatteschi, D.; Tsukerblatt, B. S.; Doring, J.; Müller, A.; Brunel, L. C. *Inorg. Chem.* **1992**, *31*, 5132−5134.

S0020-1669(96)00226-1 CCC: $12.00

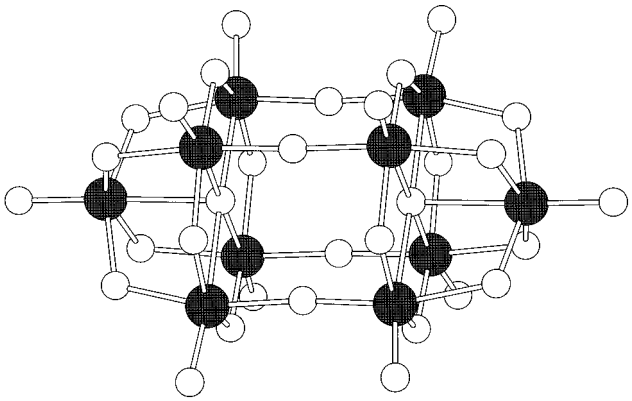

Figure 1. Ball-and-stick representation of $[W_{10}O_{32}]^{4-}$, **1**. W and O atoms are solid and open circles, respectively.

Lindquist fragment is composed of five tungsten-centered octahedra. Four octahedra are edge-shared within a plane (equatorial sites), and the fifth octahedron is edge-shared to all four equatorial tungsten atoms (axial site). The D_{4h} symmetry of **1** indicates two distinct groups of tungsten centers: eight equivalent equatorial sites and two equivalent axial sites. The structure of the d^0 Wells−Dawson heteropolytungstate of approximate D_{3h} symmetry α-$[P_2W_{18}O_{62}]^{6-}$ (structure not shown) consists of two defect A-PW_9 fragments derived from the Keggin PW_{12} structure which are linked by six nearly linear W−O−W bonds.[47−49] Each A-PW_9 fragment consists of three axial site edge-shared octahedra which are each corner-shared to one pair of the six equatorial octahedra. The six equatorial octahedra form a loop alternately sharing edges and corners. The D_{3h} symmetry of α-$[P_2W_{18}O_{62}]^{6-}$ indicates two different groups of tungstens: twelve equivalent equatorial sites and six equivalent axial sites. In the two-electron-reduced Wells−Dawson heteropolytungstate α-$[P_2W_{18}O_{62}]^{8-}$, it was shown that the d electrons are located primarily on the equatorial sites as similarly concluded for the singly-reduced complex α-$[P_2W_{18}O_{62}]^{7-}$.[10,13] The one-electron-reduced complex of **1**, $[W_{10}O_{32}]^{5-}$, was prepared previously by controlled-potential reduction in *N*,*N*-dimethylformamide (DMF).[11] Additionally, a mixture of reduced decatungstate species of variable protonation and reduction state, $[H_xW_{10}O_{32}]^{(y-x)-}$ ($y = 5$ and 6 for one-electron and two-electron reduction, respectively), was prepared by UV-photolysis of a single crystal of the tetraisopropylammonium salt of **1** at low temperature. On the basis of proposed superhyperfine coupling to protons in the low-temperature ESR spectra of this photoreduced crystal, it was concluded that the d electron in $[H_xW_{10}O_{32}]^{(5-x)-}$ was found primarily on the equatorial sites.[30] Additionally, the two-electron-reduced complex of **1** $H_x[W_{10}O_{32}]^{(6-x)-}$ (H_x**2**) in an uncharacterized protonation state, *x*, was prepared previously by controlled-potential reduction in DMF;[11] however, no details on the location of the d electrons in H_x**2** were given and the synthesis of unprotonated **2** has not been reported. It should be emphasized that the state of protonation in reduced polyoxometalates may have important consequences regarding their electronic structures. For example, the following observations are general for polyoxometalates with increasing protonation state: reduction potentials exhibit large positive shifts; two monoelectronic reduction waves merge to form a single bielectronic wave; and electronic absorbance bands exhibit hypsochromic shifts.[8]

We report here the synthesis of *unprotonated* **2** prepared by the two-electron electrochemical reduction of **1** in acetonitrile and its characterization by NMR (^{17}O and ^{183}W) and UV−visible/near-IR spectroscopy. Four distinct protonated derivatives of **2**, H_x**2** ($x = 0-4$), are prepared *in situ* by addition of triflic acid. These H_x**2** species are EPR silent over 4−300 K and are effectively diamagnetic. Also given are the full experimental protocols for acquisition of both high signal-to-noise and integrable natural-abundance ^{17}O NMR spectra of polyoxometalates, which are now made possible largely through the use of high-field magnets. This ability is important since enrichment with ^{17}O can lead to problems in the relative quantitation of oxygen sites.[50] Additionally, two previously unobservable ^{17}O NMR resonances of **1** are assigned and reported here.[51] Both the ^{17}O and ^{183}W NMR spectra of **2** are consistent with retention of the structure of **1** and demonstrate that the two d electrons are delocalized on the NMR time scale. An analysis of ^{17}O line widths indicates an enhanced covalence among the three types of μ_2-W−O−W bridging bonds in **2** relative to those in **1**. Importantly, both ^{183}W NMR chemical shift and T_1 measurements indicate that the two d electrons in **2** are located primarily on the eight equatorial sites. Consequently, **2** and α-$[P_2W_{18}O_{62}]^{8-}$ are the only diamagnetic W^V-site "pure-addenda" (isometal) polyoxometalates characterized to date that exhibit an asymmetric d-electron distribution among the metal sites.

Experimental Section

Materials. The tetra-*n*-butylammonium (henceforth Q) salt, QBr (Aldrich), 1.00 M QOH in methanol (Aldrich), phenolphthalein (Aldrich), and $Na_2WO_4 \cdot 2H_2O$ (AESAR) were commercial samples and were used as received. Triflic acid (Aldrich, 99%) was stored under dry argon and used without further purification. Acetonitrile was UV-spectrophotometry grade obtained from Burdick & Jackson (<0.001% water) and was stored over activated 3 Å molecular sieves under an argon atmosphere. For electrolysis, the acetonitrile also was stored in a N_2-filled glovebox. The supporting electrolyte, QPF_6 (Bioanalytical Systems, BAS), was recrystallized once from either acetonitrile or dichloromethane. The complex $Q_4[W_{10}O_{32}]$, **1**, was synthesized by a published procedure with minor modifications in the purification step.[11,45] Both **1** and the supporting electrolyte QPF_6 (Bioanalytical Systems) were dried rigorously on a vacuum line at 90 °C for 12 h prior to electrochemical experiments.

Electrochemistry. All controlled-potential electrolyses and subsequent product manipulations were performed in a N_2-filled glovebox. The homemade three-compartment electrolysis cell (H-configuration) was similar in design to that reported by Smith and Bard.[52] The design allowed for minimal *IR* drop, rapid electrolysis (mass transfer rate constant $k = 5.97 \times 10^{-3}$ s^{-1}), maximal separation of cathode/anode products, and monitoring of products by both cyclic voltammetry and coulometry. A segment of carbon cloth (Electrosynthesis), a glassy

(39) Gatteschi, D.; Tsukerblatt, B.; Barra, A. L.; Brunel, L. C.; Müller, A.; Doring, J. *Inorg. Chem.* **1993**, *32*, 2114−2117.
(40) Gatteschi, D.; Tsukerblat, B. *Mol. Phys.* **1993**, *79*, 121−143.
(41) Borrás-Almenar, J. J.; Clemente, J. M.; Coronado, E.; Tsukerblat, B. S. *Chem. Phys.* **1995**, *195*, 1−15.
(42) Borrás-Almenar, J. J.; Clemente, J. M.; Coronado, E.; Tsukerblat, B. S. *Chem. Phys.* **1995**, *195*, 17−28.
(43) Borrás-Almenar, J. J.; Clemente, J. M.; Coronado, E.; Tsukerblat, B. S. *Chem. Phys.* **1995**, *195*, 29−47.
(44) Coronado, E.; Gómez-García, C. J. *Comments Inorg. Chem.* **1995**, *17*, 255−281.
(45) Duncan, D. C.; Netzel, T. L.; Hill, C. L. *Inorg. Chem.* **1995**, *34*, 4640−4646.
(46) Fuchs, J.; Hartl, H.; Schiller, W.; *Acta Crystallogr., Sect. B: Struct. Sci.* **1976**, *B32*, 740−749.
(47) Strandberg, R. *Acta Chem. Scand.* **1975**, *A29*, 350−358.
(48) D'Amour, H. *Acta Crystallogr., Sect. B: Struct. Sci.* **1976**, *B32*, 729.
(49) Dawson, B. *Acta Crystallogr., Sect. B: Struct. Sci.* **1953**, *B6*, 113.
(50) Site-selective enrichment of polyoxometalate oxygens by exchange with water oxygen has been observed.[51]
(51) Filowitz, M.; Ho, R. K. C.; Klemperer, W. G.; Shum, W. *Inorg. Chem.* **1979**, *18*, 93−103.
(52) Smith, W. H.; Bard, A. J. *J. Am. Chem. Soc.* **1975**, *97*, 5203−5210.

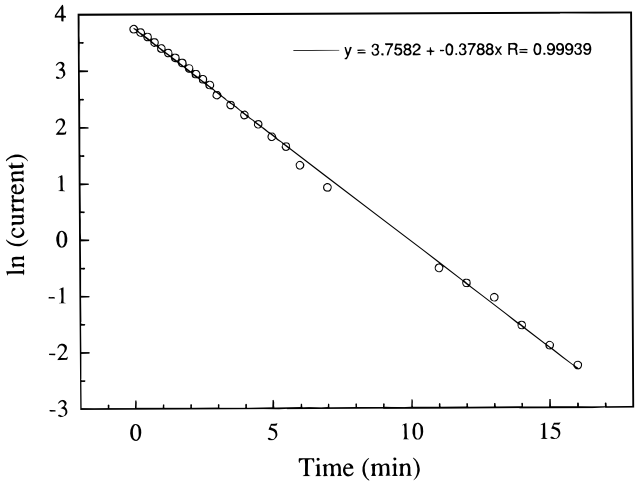

Figure 2. Plot of the natural logarithm of current versus time for the two-electron-reductive electrolysis of 5 mM $Q_4[W_{10}O_{32}]$ (**1**) in 0.5 M QPF_6 acetonitrile solution.

carbon disk (BAS), a platinum coil, and a Luggin capillary containing 0.01 M $AgNO_3$/Ag in supporting electrolyte (100-fold molar excess of QPF_6 in CH_3CN) served as the working electrode (electrolysis), working electrode (cyclic voltammetry), auxiliary electrode, and reference electrode, respectively. Cyclic voltammograms were recorded on either a Bioanalytical Systems (BAS) CV-137 instrument or a Princeton Applied Research (PAR) apparatus consisting of a PAR 174 potentiostat, a PAR 175 universal programmer, a PAR 176 current follower, and a Houston Instruments X-Y recorder. Both controlled-potential electrolyses and coulometry were performed with the BAS system for [**1**] ≤ 5 mM and with the PAR apparatus for [**1**] > 5 mM. The digital charge-integrating mode was used for coulometry with the BAS system whereas graphical integration of current vs time plots was necessary to quantify charge using the PAR apparatus. Control experiments on electrolysis of the supporting electrolyte solution alone showed a sensitivity of the reduction potential window to the presence of small quantities of water. Consequently, all efforts were made to keep materials scrupulously dry (see Materials). The resulting H_2O concentration was not measured; however, we estimate it to be <0.001% H_2O. This allowed the reduction potential window to be increased from −1.8 to −2.25 V and allowed a linear plot of ln(current) vs time to be obtained for the preparation of **2** at −2.2 V (Figure 2). The base of the irreversible wave at −2.25 V is most likely due to the half reaction $2H_2O \rightarrow H_2 + 2OH^-$. In this regard, platinum was found to be an unsuitable material for the electrolysis of decatungstate because of the low overpotential for hydrogen generation. Indeed, the second wave is irreversible using platinum whereas it is totally reversible on graphite thread or glassy carbon. Solutions of **2** stored for 1 year both within a Schlenk flask and inside a glovebox exhibited no changes in spectral characteristics. The one-electron-reduced complex, $[W_{10}O_{32}]^{5-}$ (**3**), was synthesized from an acetonitrile solution 5 mM in **1** at −1.47 V. Preparation of **2** for NMR experiments was performed by starting with an acetonitrile solution 5 mM in **1** and 0.5 M in QPF_6 electrolyte while the cathode compartment was continually fed with additional **1** each time the current dropped to 10% of the initial value. The resulting solution was 0.04 M in **2**. Additionally, NMR samples prepared by concentrating acetonitrile solutions initially 5 mM in **2** and 0.5 M in QPF_6 to ∼0.04 M in **2** gave similar NMR and UV−visible/near-IR spectra. Repeated attempts to isolate **2** devoid of electrolyte from any of these solutions failed.

Titration of 2 with Triflic Acid. An approximately 0.1 M triflic acid solution in anhydrous acetonitrile was prepared and manipulated in a round-bottom flask equipped with a venting stopcock and glass stopper while both water and oxygen were rigorously excluded with a stream of dry argon. This solution was standardized by titration with a 1.00 M methanol solution of QOH using phenolphthalein as an endpoint indicator. Inside the glovebox, 2.0 mL of an acetonitrile solution 5 mM in **2** and 0.5 M in QPF_6 was placed in a 0.1 mm path length quartz spectrophotometer cell fitted with a Teflon stopcock and a side arm for degassing which was fitted with a rubber septum. Outside the box, the requisite equivalents of triflic acid were delivered to the solution by syringe under dry argon, and the UV−visible/near-IR spectra were recorded. Due to the frequent sampling of the triflic acid solution, its concentration was checked by base titration during the course of experiments.

EPR and Electronic Absorbance Spectra. EPR spectra were recorded on acetonitrile solution samples at X-band with a Bruker ER200D spectrometer equipped with a helium cryostat. Electronic absorbance spectra (UV−visible/near-IR) were recorded on a Shimadzu UV-3101PC instrument in quartz cells sealed with Teflon stopcocks.

High Signal-to-Noise (S/N) Natural-Abundance ^{17}O NMR Spectra. Such spectra have not been generally applicable to or effective for polyoxometalates; ^{17}O isotopic enrichment has been required for acquisition of satisfactory ^{17}O NMR spectra of these complexes.[51,53−56] The following data acquisition and other experimental parameters facilitate rapid and quite respectable (high S/N) ^{17}O NMR spectra.

The NMR spectral measurements were recorded using a General Electric GN 10-mm high-band probe (50−203 MHz, ^{31}P-^{15}N; 90° pulse width = 50 μs for ^{17}O in H_2O-D_2O) on a General Electric GN-500 spectrometer equipped with a variable-temperature controller and interfaced with a Nicolet 1280 data system. The spectrometer was operated at 67.82 MHz (11.75 T) in the quadrature detection mode, locked on the ^2H resonance of CD_3CN (Cambridge Isotopes, 99.7 atom %) and referenced to 50:50 (v:v) H_2O-D_2O at 22 °C by the sample replacement method. Chemical shifts downfield from the reference are reported as positive ($+\delta$). The data were collected in double precision. In this manner, millions of scans could be acquired without memory overflow or compromising the digitizer resolution. The data were processed by applying an exponential apodization function and zero-filling once prior to Fourier transformation. No baseline correction was applied to any of the spectra. The error associated with chemical shift values was assessed to be not greater than 1 ppm for line widths <200 Hz and not greater than 3 ppm for line widths >200 Hz. The receiver gate and preacquisition delay parameters were set to minimize pulse breakthrough and/or amplifier and filter delays. Such phenomena contribute to a rolling baseline and obscure the NMR signals. In addition, these parameters were set without loss of any data points at the beginning of the FID and no points were removed prior to Fourier transformation as is commonly necessary to improve the spectral baseline. Further improvement in spectral quality was obtained by heating the probe to 65 °C, thereby reducing both the solution viscosity and the correlation time for molecular rotation.[51]

Precluding chemical exchange, the dominant mechanism for nuclear relaxation in ^{17}O NMR is quadrupolar relaxation; thus, for rapid molecular tumbling, the condition $T_1 \cong T_2$ holds.[57−61] As a consequence, we found it possible to collect up to hundreds of scans per second, thereby permitting natural-abundance spectra to be obtained in only a few hours. The optimal acquisition time is found by measuring the reciprocal line width of the narrowest line in the spectrum which corresponds to T_2*, the effective transverse relaxation time. Due to the broad resonances from ^{17}O nuclei, T_2* can be equated with the true transverse relaxation time, T_2. Setting the acquisition time to at least $4T_2$ allows for recovery of more than 98% of the signal intensity. This acquisition time provides the optimal balance of resolution, maximum S/N for a given FID, and the need for accurate peak integrations. In the acquisition of high-quality spectra suitable for peak integration, typically 10^6 transients are accumulated (∼4.5 h). However,

(53) Besecker, C. J.; Klemperer, W. G.; Maltbie, D. J.; Wright, D. A. *Inorg. Chem.* **1985**, *24*, 1027−1032.
(54) Klemperer, W. G.; Schwartz, C.; Wright, D. A. *J. Am. Chem. Soc.* **1985**, *107*, 6941−6950.
(55) Day, V. W.; Klemperer, W. G.; Maltbie, D. J. *J. Am. Chem. Soc.* **1987**, *109*, 2991−3002.
(56) Day, V. W.; Eberspacher, T. A.; Klemperer, W. G.; Park, C. W.; Rosenberg, F. S. *J. Am. Chem. Soc.* **1991**, *113*, 8190−8192.
(57) Kintzinger, J. *NMR* **1981**, *17*, 1−64.
(58) Kintzinger, J. In *NMR of Newly Accessible Nuclei*; Laszlo, P., Ed.; Academic Press: New York, 1983; Vol. 2; Chapter 4.
(59) Butler, L. G. In *^{17}O NMR Spectroscopy in Organic Chemistry*; Boykin, D. W., Ed.; CRC Press: Boca Raton, FL, 1991; Vol. 1; Chapter 1.
(60) Gerothanassis, I. P. *Org. Magn. Reson.* **1983**, *21*, 719−722.
(61) Abragam, A. *Principles of Nuclear Magnetism*, 2nd ed.; Clarendon Press: Oxford, U.K., 1983.

the unduly large 90° pulse width of the broad-band probe provides power to only a narrow range of frequencies. In order to ensure a more even power distribution across the spectral window, a shorter pulse width (15−20 μs) had to be used at the expense of reducing the S/N. The power distribution is expected to follow a (sin x)/x dependence where $x = \pi\tau\Delta\nu$, τ is the pulse width, and $\Delta\nu$ is the carrier offset frequency.[62,63] This equation is used to correct the peak integrations.

The NMR sample of **2** was prepared as follows: To a vial was added 10 mL of a 0.04 M solution of **2** (*vide infra*), and the solvent was stripped under vacuum. The solid was taken up in deoxygenated anhydrous CD_3CN until the volume reached 4 mL (0.1 M **2**). The resulting solution was placed in a 10 mm o.d. NMR tube fitted with a J. Young valve for excluding oxygen. Additionally, identical chemical shifts were obtained by removing the acetonitrile from 40 mL of a 5 mM solution of **2** and then adding 4 mL of CD_3CN. The acquisition parameters are found in the caption of Figure 5. Additionally, a calibrated Cannon−Fenske type viscometer (Fisher) was used to measure the kinematic viscosities at 65 °C for both an acetonitrile solution 0.12 M in **1** and one saturated in QPF_6 (13 g in 9 mL). Such a measurement on a solution 0.1 M in **2** and ∼1.25 M in QPF_6 was obviated by the necessity to exclude O_2; consequently, the viscosity of the saturated QPF_6 solution was used as an upper limit for that of **2**.

^{183}W NMR. NMR spectral measurements were recorded at 20.84 MHz (11.75 T) using a General Electric GN 10-mm low-band probe (12−104 MHz, ^{177}Hf−^{127}I; 90° pulse width = 47.5 μs for Na_2WO_4 in D_2O) on the same General Electric GN-500 spectrometer used to acquire ^{17}O spectra. Chemical shifts are referenced by the sample replacement method to Na_2WO_4 in D_2O (Cambridge Isotopes, 99.9 atom %) adjusted to pD = 10 with NaOH. The sample preparation procedures were identical with those described for the ^{17}O measurements. Note that both procedures for the NMR sample preparation gave identical chemical shifts. Acquisition parameters and sample conditions are found in the caption of Figure 4.

Results and Discussion

Synthesis and Electrochemistry. The two-electron-reduced isopolyanion H_x**2** has been prepared previously in *N*,*N*-dimethylformamide (DMF) as the tri-*n*-butylammonium salt with the addition of a proton donor.[11] We report here the synthesis of **2** prepared by controlled-potential electrolysis in the absence of protic media (see Experimental Section). The cyclic voltammogram of **2** is identical with that of the starting material **1** and consists of two reversible single-electron redox couples with formal potentials of −1.2 and −1.8 V vs 0.01 M $Ag/AgNO_3$ in 0.1 M QPF_6 anhydrous acetonitrile solution.[64] Coulometric monitoring of the electrolysis indicates the addition of 2.00 mol equiv of electrons to **1**. Additionally, cleanness of the electrolysis is demonstrated in Figure 2, which shows linearity over more than 5 orders of magnitude in a plot of the natural logarithm of current versus time.

Electronic Spectroscopy. The UV−visible/near-IR spectrum of **2** is shown in Figure 3a and contains two principal band features located at 668 and 1191 nm with extinction coefficients of 14 000 and 10 300 M^{-1} cm^{-1}, respectively. These molar absorptivities are similar to those reported previously for H_x**2** in DMF at 630 and 970 nm, respectively.[11] Furthermore, the values for **2** are approximately twice those of the corresponding electronic transitions in the one-electron-reduced complex, **3**, which are located at 780 nm (7000 M^{-1} cm^{-1}) and 1555 nm (4500 M^{-1} cm^{-1}) in acetonitrile.[65] Additionally, each of the two bands for **2** exhibit a similar blue shift with respect to the corresponding bands for **3**: 0.244 eV (1555 → 1191 nm) and 0.266 eV (780 → 668 nm). These data suggest that the nature of the electronic transitions responsible for these bands is invariant on reducing **3** to **2**, and they rule out the existence of a W^{IV} site. The previous assignment of the 1555-nm band of **3** as an intervalence transition implies a similar intervalence nature for the 1191-nm band of **2**. However, the origin of the 780-nm band of **3** and the corresponding band of **2** at 668 nm is not well understood.[11] Additionally, the 370-nm band of **3** disappears altogether in the spectrum of **2**. If this transition remains for **2**, then it must be blue-shifted by at least 0.78 eV with respect to that of **3**.

Table 1. Electronic Absorbance Data for $H_x[W_{10}O_{32}]^{(6-x)-}$ (x = 0−4) in CH_3CN[a]

compd	λ, nm (ϵ, M^{-1} cm^{-1})[b]
2	1191 (10 300); 1070 s (6100); 844 s (2700); 668 (14 000); 628 s (12 100); 279 s (11 900)
H**2**	1058 (10 000); 753 s (6200); 642 (13 600); 574 s (7100); 276 s (11 900)
H_2**2**	958 (13 500); 777 s (7400); 695 s (10 100); 625 (13 600); 519 s (4500); 302 s (4400); 276 s (11 900)
H_3**2**	921 (14 200); 668 s (13 300); 621 (16 100); 509 s (4600); 278 s (11 900)
H_4**2**	881 (14 600); 618 (16 500); 482 s (3400); 278 s (11 900)

[a] Spectra along with conditions are shown in Figure 3. [b] Extinction coefficients were obtained from absorbances corrected both for volume of acid titer added and for the small amount of $[W_{10}O_{32}]^{5-}$, **3**, generated *via* adventitious O_2 (<5%) which was quantified by the small absorbance increase at 370 nm. The reduction potentials shift to more positive values with protonation, and consequently only the x = 0−2 forms of H_x**2** are markedly air-sensitive.

On protonation, marked changes occur in the UV−visible/near-IR spectra of **2**. The titration of an acetonitrile solution 5 mM solution in **2** with an acetonitrile solution 0.13 M in triflic acid (Figure 3) shows clean isosbestic behavior in each of four successively higher acid concentration ranges, consistent with five distinct protonation states, H_x**2** (x = 0−4). The absorbance maxima and molar absorptivities for the five reduced species are given in Table 1. The two principal band components of **2** with their respective shoulders all blue-shift on successive protonation. The 1191-nm band of **2** is markedly asymmetric and increases both in bandwidth and in Gaussian character on protonation. However, the resulting 881-nm band of H_4**2** remains asymmetric and therefore must still contain unresolved structure on the high-energy side of the band. The 668-nm band of **2** broadens substantially on protonation to H_2**2**; further protonation results in a relatively symmetric band for H_4**2** whose width is close to that for **2**. Additionally, a new band appears as a shoulder at 574 nm for H**2** and blue-shifts on successive protonations ending at 482 nm for H_4**2**. Since it is well-known that protonation shifts the reduction potentials in the ground state of **1** to more positive values (this is generally true for all polyoxometalates),[2,64] the blue shifts in the electronic spectra of H_x**2** likely arise principally when the absolute energy of the occupied molecular orbitals is lowered. The observed blue shift in the charge transfer band of **1** in the presence of triflic acid (324 → 318 nm) corroborates this point.

^{183}W NMR and EPR. No EPR signals were detected from acetonitrile solutions of **2** over the temperature range 4−298 K. This lack of an observable EPR signal for **2** indicates the

(62) Brevard, C. In *NMR of Newly Accessible Nuclei*; Laszlo, P., Ed.; Academic Press: New York, 1983; Vol. 1; Chapter 1.
(63) Appelman, E. H.; Kostka, A. G.; Sullivan, J. C. *Inorg. Chem.* **1988**, *27*, 2002−2005.
(64) Renneke, R. F.; Pasquali, M.; Hill, C. L. *J. Am. Chem. Soc.* **1990**, *112*, 6585−6594.

(65) The one-electron-reduced complex, $[W_{10}O_{32}]^{5-}$ (**3**), has been prepared previously in DMF.[11] The UV−visible/near-IR spectrum of **3** in acetonitrile has been published and is identical to that reported in DMF.[45]

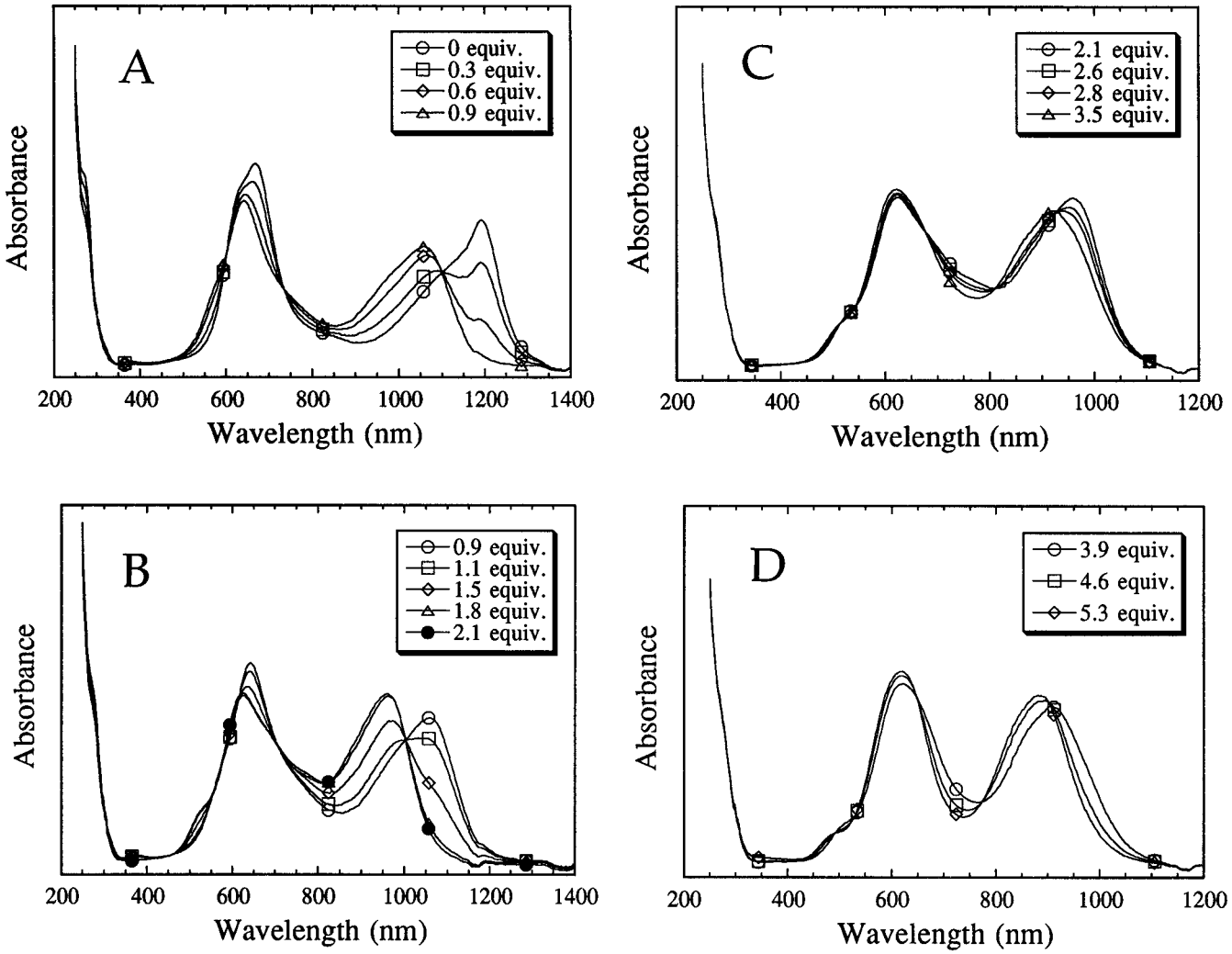

Figure 3. UV−visible/near-IR spectra of an acetonitrile solution 5 mM in $[W_{10}O_{32}]^{6-}$ (**2**) and 0.5 M in QPF_6 which was titrated with an acetonitrile solution 0.13 M in triflic acid. The molar equivalents of H^+ added are based on **2**. (A) 0−0.9 equiv of H^+; (B) 0.9−2.1 equiv of H^+; (C) 2.1−3.5 equiv of H^+; (D) 3.9−5.3 equiv of H^+. Cell path length is 0.1 mm. See Experimental Section for further details. The small peak at 370 nm in parts A and B is due to generation of **3** (<5% conversion) by adventitious O_2.

ground-state is effectively diamagnetic, and hence the NMR signals for nuclei which are directly populated by the d electrons become observable. The ^{183}W NMR data for both **1** and **2** are shown in Figure 4 and Table 2. The chemical shifts for **1** appear at −22.5 and −165.6 ppm for the equatorial and axial tungstens, respectively. The ^{183}W chemical shifts for **2** are found at +307 and −149 ppm which integrate 4:1 corresponding to the equatorial and axial tungstens, respectively. The existence of only two ^{183}W resonances in the expected integrated ratio confirms retention of both the structure and overall D_{4h} symmetry on reducing **1** by two electrons. Consequently, the d electrons are "delocalized" on the ^{183}W NMR time scale. Additionally, ^{183}W T_1 measurements were performed on both the equatorial and axial sites in **2**. The T_1 measured for the equatorial tungstens is 12.7 ± 0.1 ms. However, a reliable T_1 measurement for the axial sites was obviated by the slight oxidation of the sample over the time required for the measurement (several days). Our efforts indicate a T_1 range of 42 ms $\leq T_1 \leq$ 100 ms, although the 100 ms value is the most likely. The partial oxidation was indicated both by a broadening of each ^{183}W NMR resonance and by a decrease in each T_1; however, no changes in the chemical shifts were observed.

Two lines of evidence derived from the ^{183}W NMR data indicate that the two d electrons in **2** are located primarily on the *equatorial* sites. First, Kozik and Baker have shown a correlation between large positive ^{183}W shift changes ($\Delta\delta >$ +100 ppm where $\Delta\delta = \delta_{reduced} - \delta_{oxidized}$) and d-electron density for a given tungsten site in diamagnetic polyoxotungstate blue complexes.[13] The shift change for the equatorial sites in **2**, + 329.5 ppm, is larger than that reported for any other "pure-addenda" (isometal) W^V-site polyoxotungstate to date.[66] The magnitude of the shift is intriguing; unfortunately, however, the origin of ^{183}W shifts for reduced diamagnetic polyoxometalates remains uncertain.[67] A thorough experimental and theoretical investigation in this area could provide detailed information on the mixed-valence properties of diamagnetic polyoxotungstates. Second, Kozik and Baker also reported an inverse correlation between the d-electron density at a tungsten site and its ^{183}W T_1.[13] The enhanced nuclear relaxation observed in the diamagnetic reduced complexes likely derives from modulation of the

(66) Heteropolybrown complexes exhibit even larger shift changes (>1000 ppm).[25] However, the origin of the shifts in heteropolybrown complexes probably reflects an anomalous π-contribution arising from the localized $W^{IV}-W^{IV}$ metal−metal bonding (see: Kidd, R. G. In *Annual Reports on NMR Spectroscopy*; Webb, G. A., Ed.; Academic Press: New York, 1982; Vol. 23, pp 85−140). This mechanism is not operative for polyoxoblue complexes unless one invokes a bipolaron model where the W^V-W^V metal−metal interaction is transient.[67]

(67) For a complete analysis of reduced polyoxometalate ^{183}W chemical shifts see: Duncan, D. C. Dissertation Thesis, Emory University, 1995.

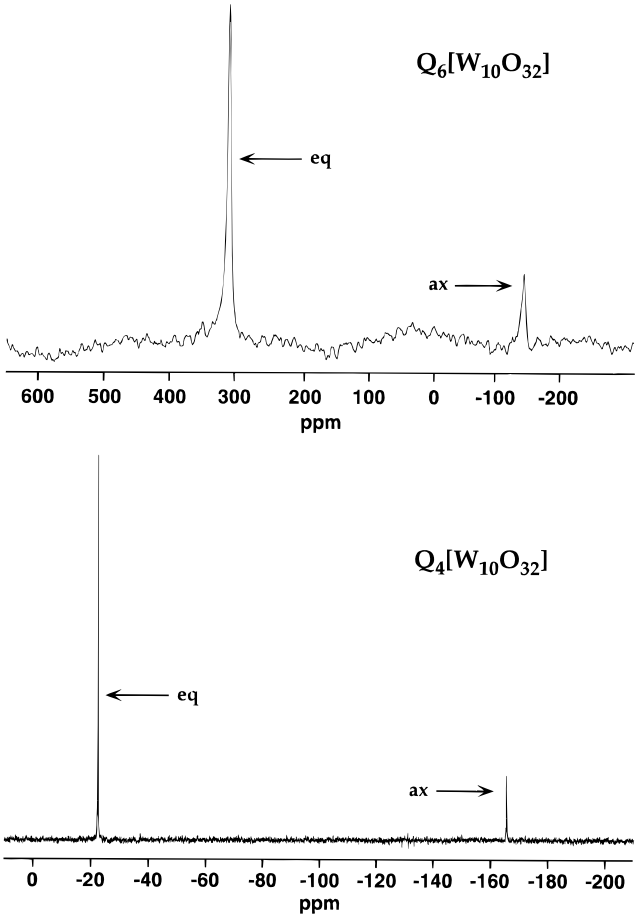

Figure 4. ^{183}W NMR spectra at 20.84 MHz in CD_3CN. Top: 0.1 M $[W_{10}O_{32}]^{6-}$, **2**, in ~1.25 M saturated QPF_6/CD_3CN. Parameters: pulse width = 47.5 μs; relaxation delay = 100 ms; block size (double precision) = 8K; acquisition time = 102.4 ms; dwell time = 50 μs; receiver gate = 99 μs; preacquisition delay = 20 μs; number of acquisitions = 114 128; temperature = 22 °C. Bottom: 0.12 M $Q_4[W_{10}O_{32}]$, **1**, in CD_3CN. Parameters: pulse width = 47.5 μs; relaxation delay = 12 s; block size = 16K; acquisition time = 1.36 s; dwell time = 166 μs; receiver gate = 160 μs; preacquisition delay = 55 μs; number of acquisitions = 1000; temperature = 22 °C. A matched filter exponential function was used to apodize each FID prior to Fourier transformation. The symbols eq and ax denote equatorial and axial tungsten sites, respectively.

Table 2. ^{183}W (20.84 MHz) NMR Spectral Data for **1** and **2** in CH_3CN[a]

	δ, ppm		
tungsten site	**1**	**2**	$\Delta\delta$, ppm[b]
^{183}W equatorial	−22.5	307	329.5
^{183}W axial	−165.6	−149	16.6

[a] See Figure 4 for spectral parameters and conditions. [b] $\Delta\delta = \delta(\mathbf{2}) - \delta(\mathbf{1})$.

local magnetic field which originates in the d-electron "hopping" motion. Suitable low-frequency field components derived from the d-electron motion stimulate ^{183}W relaxation where the field amplitudes are markedly dependent on the distance from the d-electron sources. Consistent with this inverse correlation, the equatorial-site T_1 in **2** is much smaller than that measured for the axial site and therefore indicates a greater d-electron density on the equatorial sites.

^{17}O NMR. The ^{17}O NMR data for both **1** and **2** are reported in Figure 5 and Table 3. The ^{17}O chemical shifts agree with previously reported values for **1**;[51] however, a new resonance in the ^{17}O NMR centered at 732 ppm and both partial resolution and peak deconvolution for one of the overlapping resonances

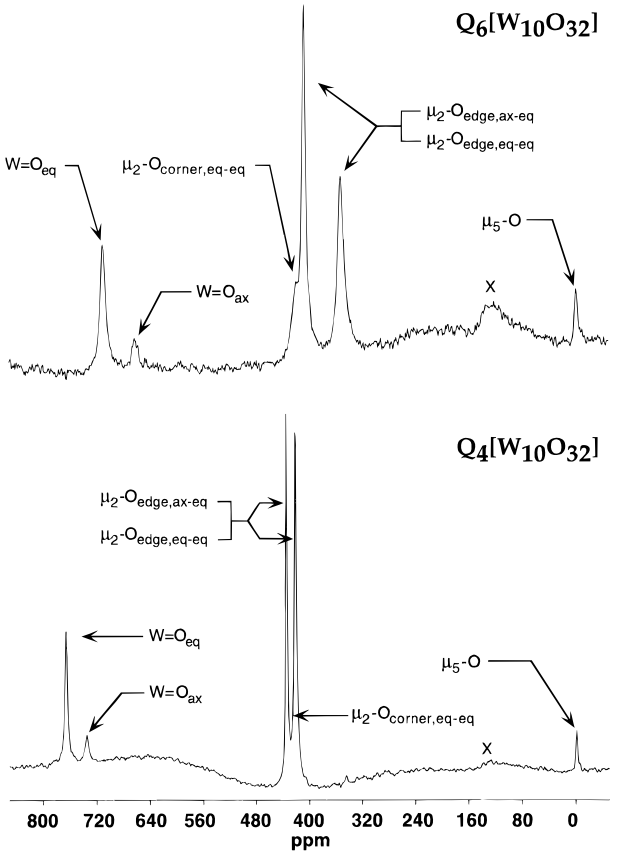

Figure 5. ^{17}O NMR spectra at 67.82 MHz in CD_3CN. Top: 0.1 M $[W_{10}O_{32}]^{6-}$, **2**, in ~1.25 M saturated QPF_6/CD_3CN. Parameters: pulse width = 20 μs; relaxation delay = 1 ms; blocksize (double precision) = 2K; acquisition time = 7.17 ms; dwell time = 14 μs; receiver gate = 13 μs; preacquisition delay = 5 μs; number of acquisitions = 4 194 304; temperature = 65 °C. Bottom: 0.12 M $Q_4[W_{10}O_{32}]$, **1**, in CD_3CN. Parameters: pulse width = 20 μs; relaxation delay = 1 ms; block size (double precision) = 4K; acquisition time = 15.36 ms; dwell time = 15 μs; receiver gate = 14 μs; preacquisition delay = 3 μs; number of acquisitions = 1 048 576; temperature = 65 °C. The broad peaks at ~135 ppm (labeled ×) also are observed without a sample in the probe; they are artifacts. A matched filter exponential function was used to apodize each FID prior to Fourier transformation. The symbols eq and ax denote equatorial and axial tungsten sites respectively.

are reported here for the first time.[68] There are two types of terminal oxygens (two axial and eight equatorial), three types of μ_2-bridging oxygens (eight μ_2-edge-sharing which link the axial and equatorial tungstens, eight μ_2-edge-sharing between the equatorial tungstens, and four μ_2-corner-sharing which link the two W_5 fragments), and one type of two central μ_5-oxygens

(68) The new resonance at 732 ppm bears further comment. This peak was not observed in the previously reported ^{17}O-enriched spectrum of this compound.[51] In our work, efforts were made to determine the origin of this resonance (impurity, decomposition, etc.). The possibility of decomposition due to heating the sample was ruled out by first recording the spectrum at 22 °C. On heating of the sample to 65 °C, no new features appeared in the spectrum and the relative peak integrals for the 765 and 732 ppm peaks remained the same. In addition, on cooling of the sample back to 22 °C, the same results were obtained. Furthermore, ^{183}W NMR (18 821 scans at 4.74 T) and cyclic voltammetry confirmed the purity of the sample. As a further check, multiple recrystallizations revealed no changes in the spectra. We are not sure why this resonance was not observed for the enriched sample in the aforementioned earlier report; however, it is possible that under those experimental conditions (^{17}O Larmor frequency = 13.51 MHz; higher viscosity and therefore larger line widths), the small broad resonance could not be observed in the presence of the large peak. It is also possible that the signal was below the discriminator level of the digitizer. Further evidence in support of the 732 ppm assignment follows from the symmetric line shape observed for the 765 ppm resonance and from the peak integrations.

Table 3. ^{17}O (67.82 MHz) NMR Spectral Data for **1** and **2** in CH_3CN[a]

oxygen site	δ, ppm ($\Delta\nu_{1/2}$, Hz; integral)[a,b] **1**	**2**	$\Delta\delta$, ppm ($\Delta\nu_{1/2}$(**2**)/$\Delta\nu_{1/2}$(**1**))
^{17}O═W eq	765 (190; 8.0)	709 (550; 7.9)	-56 (2.9)
^{17}O═W ax	732 (380; 1.8)	662 (530; 1.7)	−70 (1.4)
μ_2-^{17}O edge-shared	434 (58; 8.0)[d]	405 (660; 8.0)[d]	−16 (6.5), −85 (18)
(eq−eq and ax−eq)[c]	421 (102; 7.6)[d]	349 (1040; 7.5)[d]	or −29 (11), −72 (10)
μ_2-^{17}O corner-shared	423 (263; 4.0)[d]	419 (1490; 4.3)[d]	−4 (5.7)
μ_5-^{17}O central	−1.6 (90; 2.2)	−2.4 (240; 1.8)	−8 (2.7)

[a] See Figure 5 for spectral parameters and conditions. [b] Reported line widths were corrected for exponential apodization (matched filter) and the peak integrals were corrected for uneven pulse power distribution. See Experimental Section. [c] It is not yet possible to distinguish unambiguously between the two ^{17}O resonances responsible for the two μ_2-edge-sharing oxygen types (eq = equatorial, ax = axial). [d] Peak deconvolution was performed using Felix NMR software.

(Figure 1). On the basis of peak integrations and the known correlation of downfield chemical shift with increasing bond order, the two resonances at 765 and 732 ppm are assigned to the equatorial and axial terminal oxygens, respectively.[51,69] The 434 and 421 ppm resonances are assigned to the three types of μ_2-bridging oxygens which integrate to eight and twelve oxygens, respectively. Consequently the 421 ppm resonance must be a convolution of the four μ_2-corner-sharing oxygens and *either* of the two types of eight μ_2-edge-sharing oxygens. This conclusion is confirmed by close inspection of the line shapes. The 434 ppm resonance is symmetric whereas the 421 ppm resonance is markedly asymmetric with a broad tail toward the low-field side of the resonance. Deconvolution of this asymmetric band using Lorentzian line shapes yields two peaks with a 2:1 area ratio. The four μ_2-corner-sharing oxygens are assigned to the broad resonance centered at 423 ppm determined from the deconvolution. It is not yet possible to distinguish unambiguously between the two types of μ_2-edge-sharing oxygen resonances (axial−equatorial and equatorial−equatorial). The two central μ_5-oxygens are assigned to the resonance at −1.6 ppm in accord with the previous report.[51]

On reduction of **1** to **2**, six peaks remain with satisfactory integrations, indicating that the anion has retained its structure and overall D_{4h} symmetry. Using the same arguments as before, the peaks due to the terminal equatorial and axial oxygens are found at 709 and 662 ppm, respectively. The resonance due to the four μ_2-corner-sharing oxygens is partially resolved at 419 ppm. Again it is not possible to determine unambiguously the identity of the two resonances located at 405 and 349 ppm other than that they are due to the two types of μ_2-edge-sharing oxygens. The peak at −2.4 ppm is assigned to the two central μ_5-oxygens. All of the chemical shifts for **2** have been shifted upfield with respect to **1**. The magnitude of these shifts is particularly large for both the terminal oxygens and one of the μ_2-edge-sharing oxygens.

^{17}O nuclear magnetic relaxation is dominated by interaction of the nuclear quadrupole moment with the electric field gradient surrounding the nucleus. This relaxation rate is described in eq 1, where T_1 and T_2 are the longitudinal and transverse

$$\frac{1}{T_1} = \frac{1}{T_2} = \frac{3}{125}\left(1 + \frac{\eta^2}{3}\right)\left(\frac{2\pi e^2 Q q_{zz}}{h}\right)^2 \tau_c \qquad (1)$$

$$\eta = \frac{eq_{xx} - eq_{yy}}{eq_{zz}} \qquad |eq_{zz}| \geq |eq_{yy}| \geq |eq_{xx}|$$

relaxation times respectively, η is the asymmetry parameter ($0 \leq \eta \leq 1$), Q is the nuclear electric quadrupole moment, and q is a component of the electric field gradient tensor.[61,70−72] The spectral density which modulates the interaction is often simplified to a single term, τ_c, which is the isotropic rotational correlation time. The quantities in parentheses are collectively termed the quadrupole coupling constant. Additionally, since $T_1 \approx T_2$ and $T_2 = (\pi\Delta\nu_{1/2})^{-1}$ where $\Delta\nu_{1/2}$ represents the full line width at half of the maximum peak height, the line width is a direct measurement of T_1. Provided that the molecular correlation function (*i.e.* spectral density) is known, the principal electric field gradient (efg) at an oxygen site can be estimated from a T_1 measurement, and hence information concerning the local electronic structure at oxygen can be deduced. The relative efg between two *different* oxygen sites (a and b) in the same molecule can be obtained from ^{17}O line width ratios without precise knowledge of the correlation function so long as it is isotropic. The anisotropy of the molecular rotation precludes such an analysis for either **1** or **2**; however, the line width ratio, O_a(**2**)/O_a(**1**), provides a means of deducing the resulting efg difference for the *same* oxygen site *a* between the two complexes. This is true, strictly provided that the solutions of **1** and **2** have the same viscosity and that the extreme narrowing condition holds. Although a viscosity measurement of the **2** solution (0.1 M in **2** and ∼1.25 M in QPF_6) was obviated by its sensitivity to O_2, its viscosity is unlikely to be greater than that of an acetonitrile solution saturated in QPF_6 (13 g in 9 mL). The relative kinematic viscosity of this QPF_6 solution to one 0.12 M in **1** at the temperature of the NMR measurements, 65 °C, is only 2.6. Consequently, it is concluded that the differences in line width ratios, O_a(**2**)/O_a(**1**) (final column in Table 3), for the three types of μ_2-bridging oxygens are too large to be due to differences in spectral density alone. Rather, they reflect an increase in efgs for the μ_2-bridging oxygen sites on reducing **1** to **2**. Increases in efgs at oxygen are interpreted generally *via* the Townes−Dailey approach.[59,73] In this model, an increase in bond covalency is indicated by an increase in the efg at oxygen. Consequently, the increased efg for the μ_2-bridging oxygens in **2** relative to **1** is consistent with an increased covalency among the W−O−W bonds. Interestingly, for a series of first-row transition-metal-substituted Keggin polyoxometalate complexes, Baker and co-workers have demonstrated decreases in the transition-metal spin−orbit couplings when these complexes are reduced by two electrons. The authors

(69) The W═O bond lengths are different for the equatorial and axial sites as revealed by a crystal structure determination: W═O_{axial} is 1.76 Å; W═$O_{equatorial}$ is 1.70 Å. See ref 46.

(70) Boere, R. T.; Kidd, R. G. In *Annual Reports on NMR Spectroscopy*; Webb, G. A., Ed.; Academic Press: New York, 1982; Vol. 13, pp 319−385.
(71) Kidd, R. G. In *NMR of Newly Accessible Nuclei: Chemical and Biochemical Applications*; Laszlo, P., Ed.; Academic Press: London, 1983; Vol. 1, pp 103−131.
(72) Canet, D.; Robert, J. B. In *NMR at Very High Field*; Robert, J. B., Ed.; Springer-Verlag: Heidelberg, Germany, 1991; Vol. 25, pp 45−89.
(73) Townes, C. H.; Dailey, B. P. J. *J. Chem. Phys.* **1949**, *17*, 782−796.

ascribe these decreases in spin−orbit coupling to increases in covalency, with which our results are in agreement.[19]

In summation, the reduced complex **2** exists in any one of four protonation states represented by the formula $H_x[W_{10}O_{32}]^{(6-x)-}$ ($x = 0-4$). Both the ^{183}W and ^{17}O NMR data for **2** are consistent with retention of the D_{4h} symmetry exhibited by the oxidized precursor complex **1** and that the two d electrons are delocalized on the NMR time scale. Both ^{183}W chemical shift and ^{183}W T_1 measurements indicate the two d electrons in **2** are located principally on the equatorial sites. Additionally, the ^{17}O relative electric field gradients measured by ^{17}O NMR indicate an enhanced covalency among the μ_2-W−O−W bonds in **2** relative to those in **1**. Thus **2** represents only the second example of a diamagnetic W^V-site "pure-addenda" (isometal) polyoxometalate which exhibits a marked asymmetry in d-electron distribution among the tungsten sites. Consequently, **2**, α-$[P_2W_{18}O_{62}]^{8-}$, and their singly-reduced counterparts are candidates for further exploration of mixed-valence behavior among two discrete groups of metal sites.

Acknowledgment. This research was supported by the National Science Foundation (Grant No. CHE-9412465) and the National Institutes of Health (Grant No. AI-32903). We thank Professor Thomas Netzel for the use of both the glovebox and BAS electrochemical apparatus at Georgia State University.

IC960226W